

Voigt modelling of size–strain analysis: Application to α -Al₂O₃ prepared by combustion technique

K SANTRA[†], P CHATTERJEE[‡] and S P SEN GUPTA*

Department of Materials Science, Indian Association for the Cultivation of Science, Jadavpur, Kolkata 700 032, India

[†]Department of Physics, A. P. C. College, New Barrackpore, 24-Paraganas (N) 743 276, India

[‡]Department of Physics, Vivekananda Mahavidyalaya, Haripal, Hooghly 712 405, India

MS received 4 July 2001; revised 4 March 2002

Abstract. A comprehensive analysis of size and strain broadened profile shapes in X-ray diffraction line broadening analysis is presented. Both size and strain broadened profiles were assumed to be Voigtian and the derived microstructural parameters (size and strain) were found to be in close agreement with those calculated from model independent Warren–Averbach method. The method is applied to three different alumina samples viz. micron size α -alumina (α -Al₂O₃) prepared by the combustion of aluminium nitrate and urea mixture, annealed samples and commercial α -Al₂O₃ sample. It is likely from the present analysis that a significant Gaussian size contribution is related to narrow size distribution observed from the analysis. It has been concluded that present Voigtian analysis is more reliable and may largely replace the earlier simplified integral breadth methods of analysis often used in line broadening analysis.

Keywords. X-ray diffraction; Voigt function; size–strain analysis.

1. Introduction

It is widely accepted that among the various methods used for line broadening studies, the Stokes deconvolution (Stokes 1948) method combined with the Warren–Averbach (1952) analysis is the most rigorous and unbiased approach to obtain the ‘true specimen broadened’ profile and related microstructural parameters (viz. coherent domain size, lattice microstrain etc). However, due to peak overlap and/or marginal sample broadening large errors may occur. To obtain reliable results proper corrections then have to be considered. In the simplified integral breadth method, however, the size and strain broadened profiles are assumed to be either Cauchy or Gaussian (see Balzar and Popovic 1996). It is generally assumed that size and strain broadened profiles are modelled with Cauchy and Gaussian functions, respectively. Experience shows, however, that reverse assumption of Cauchy strain and Gaussian size (Langford 1992; Balzar and Popovic 1996) often yields acceptable results. There is no standard rule for the assumption of profile shape in integral breadth methods and the choice is rather arbitrary. A general formalism was introduced by Langford (1980) and later by Balzar and Ledbetter (1993) for ‘true specimen broadened’ profile by considering both size and strain effects modelled with Voigt functions (convolution of the Cauchy and Gauss

functions). The objective of this paper is to study thoroughly the suitability of an assumed double-Voigt function in size–strain modelling. Three different α -Al₂O₃ samples hereafter designated as as-prepared, annealed and commercial are taken. Due to difference in processing history different sample characteristics is expected. Further, the volume-weighted crystallite size obtained from the double-Voigt method has also been compared with the multiple line integral breadth method using several starting assumptions for profile shapes.

2. Experimental

Micron-sized α -Al₂O₃ was prepared by the combustion of aluminium nitrate–urea mixture in the molar ratio 1 : 2.5. Redox mixture of aluminium nitrate (20 g) and urea (8 g) was dissolved in minimum quantity of double distilled water and the dish containing the solution was introduced into a furnace maintained at temperature $500 \pm 10^\circ\text{C}$. The solution boils, foams, ignites to burn with flame and produces voluminous foamy alumina powder. The as-prepared α -Al₂O₃ was further annealed at 800°C for 2 h to yield the annealed samples. A third sample of commercial α -Al₂O₃ was obtained from CGCRI, Kolkata.

X-ray powder diffraction patterns of the samples were recorded at room temperature in a Philips PW1710 diffractometer using Ni-filtered CuK α radiation operating at 35 kV and 20 mA in a step scan mode with a step size of $0.02^\circ 2\theta$ and counting time of 4 s per step.

*Author for correspondence

3. Evaluation

As regards line shape analysis of X-ray diffraction patterns of as-prepared, annealed and commercial α -Al₂O₃, the Warren–Averbach method, simplified integral breadth method and double-Voigt Fourier method were adopted to obtain the microstructural parameters. The reliability of the double-Voigt method was examined by comparing the results obtained by the other two methods. The basic expressions used in the present analysis are briefly described in the next sections.

3.1 Integral breadth method

The simplified multiple line integral breadth method generally uses either of the following equations for size–strain separation

$$b = 1/D + 2es, \quad (1)$$

$$b = 1/D + 4e^2s^2/b, \quad (2)$$

$$b = 1/D^2 + 4e^2s^2. \quad (3)$$

These three equations are denoted as Cauchy–Cauchy (or often called the Williamson–Hall plot), Cauchy–Gaussian (or intermediate parabolic) and Gaussian–Gaussian approximations where b is the integral breadth, D denotes the volume weighted domain size and e the upper limit of microstrain. The domain size and strain are generally expressed as,

$$\begin{aligned} D_{C-C}(x) &= c_1/(2-x); D_{C-G}(x) = c_1(4-x)/(4-x^2); \\ D_{G-G}(x) &= 3^{1/2} c_1/(4-x^2)^{1/2}, \end{aligned} \quad (4)$$

$$\begin{aligned} e_{C-C}(x) &= c_2(x-1); e_{C-G}(x) = c_2[x(x-1)/(4-x)]^{1/2}; \\ e_{G-G}(x) &= c_2[(x^2-1)/3]^{1/2}, \end{aligned} \quad (5)$$

where $s_2 = 2s_1$, $x = b_2/b_1$, $c_1 = 1/b_1$, $c_2 = b_1/(2s_1)$, $s = 2\sin q/l$ and $s_2 = 2s_1$. Here, the subscripts refer to first and second order of a particular reflection.

It is obvious from the above relations that for $x \geq 2$, negative or complex domain size is obtained. To perceive the absolute magnitude of domain size and strain, the comparison with the Stokes deconvolution method combined with the Warren–Averbach method is required. However, the Warren–Averbach method yields a surface weighted domain size and averaged root mean square strain (RMSS) which are not directly comparable to the volume weighted domain size and strain obtained from the integral breadth method. In special circumstances only the size and strain broadened profiles show some evidence of being of either Cauchy or Gauss type and therefore, it is reasonable to describe them with a function which is a convolution of Cauchy and Gauss functions, i.e. the Voigt function. Langford (1980) first considered both the size and strain broadened profile to be Voigt function (convolution of size and strain). A more genera-

lized treatment on that basis is possible if the Cauchy and Gaussian components of the Voigt function followed (1) and (3), respectively. The approach was used by Langford (1992) which yielded reliable results.

3.2 Separation of size and strain broadening by double-Voigt method

Balzar and Ledbetter (1993) showed that if both size and strain broadened profiles are assumed to be Voigtian the equivalent analytical expressions for Warren–Averbach size–strain separation could be obtained. As exclusively Cauchy or Gauss functions cannot satisfactorily model the specimen broadening, it is assumed that both size and strain effects are approximated by Voigt functions. The Fourier coefficients in terms of a distance, L , perpendicular to the diffracting planes is obtained by Fourier transform of a Voigt function and can be written as

$$F(L) = \exp[-2Lb_C - pL^2 b_G^2], \quad (6)$$

where, b_C and b_G are the Cauchy and Gauss components of total integral breadth b , respectively. The Cauchy and Gaussian components of the size and strain integral breadths follow the convolution principle and the following equations can be derived:

$$b_C = b_{SC} + b_{DC}, \quad (7a)$$

$$b_G^2 = b_{SG}^2 + b_{DG}^2, \quad (7b)$$

where, b_{SC} and b_{DC} are the Cauchy components of size and strain integral breadth, respectively and b_{SG} and b_{DG} are the corresponding Gaussian components.

According to Warren (1969), the total Fourier coefficients (which are products of size, F^S and distortion, F^D coefficients) can be written as

$$F(L) = F^S(L)F^D(L). \quad (8)$$

From (6), (7) and (8) we obtain

$$F^S(L) = \exp(-2Lb_{SC} - pL^2 b_{SG}^2), \quad (9a)$$

$$F^D(L) = \exp(-2Lb_{DC} - pL^2 b_{DG}^2). \quad (9b)$$

The size and distortion coefficients can be obtained considering at least two reflections from the same crystallographic plane family.

According to Warren (1969), the surface-weighted domain size is

$$[dF^S(L)/dL]_{L \rightarrow 0} = -1/D_S.$$

From (9a), it follows that

$$D_S = 1/2b_{SC}. \quad (10)$$

The volume weighted domain size is given by the expression

$$D_v = \exp(k_s^2) (1 - \operatorname{erfc}(k_s/b_{SG})), \quad (11)$$

where, k_s is a characteristic integral–breadth ratio of the size broadened Voigt profile,

$$k_s = b_{SC}/(p^{1/2}b_{SG}).$$

The distortion coefficient in harmonic approximation can be written as

$$F^D(L) = \langle \exp[2\pi i s L e(L)] \rangle \\ \cong \exp[-2p^2 s^2 L^2 \langle e^2(L) \rangle]. \quad (12)$$

Comparing (12) with (9b) we can write

$$\langle e^2(L) \rangle = [b_{DG}^2/(2p) + b_{DC}/(p^2 L)]/s^2. \quad (13)$$

The components b_{SC} , b_{DC} , b_{SG} and b_{DG} can be obtained from the total Cauchy and Gaussian breadths b_C and b_G (7) by applying (1) and (3), respectively.

4. Results

4.1 Profile fitting

α -Al₂O₃ sample produces a diffraction pattern with large number of peaks (figure 1). After inspecting the diffraction pattern it was observed that [012], [113] and [110] crystallographic direction exhibited least degree of overlapping. The analysis was thus performed for these directions only. A profile fitting methodology was used to determine the profile shape parameters and the total integral breadth for the overlapping reflections.

We have employed a pattern decomposition algorithm using a pseudo-Voigt function numerically convoluted with a truncated exponential function (Enzo *et al* 1988) to determine the integral breadths of different reflections. In our fitting process $(1-h)$, the Gaussian content and w , the half width at half maximum, the peak height, I_0 and the Bragg $2q$ position are simultaneously refined along with the parameters of the linearly varying background. The integral breadths are computed according to the relation

$$b = w[ph + (1-h)\tilde{O}p/\ln 2].$$

A well crystallized Si sample was used for instrumental broadening correction. The pattern for standard Si is also shown in figure 1. Using a position constrained whole pattern fitting (WPF) algorithm (Luterotti and Scardi 1990) the integral breadths at required $2q$ values were obtained. The equivalent Cauchy and Gaussian components of the integral breadths of the true specimen broadened profile obtained after deconvolution (de Keijser *et al* 1982) is listed in table 1.

It is clear from table 1 that for both as-prepared and annealed α -Al₂O₃ samples the profiles are Voigtian in nature for all the crystallographic directions considered

(e.g. [012], [110] and [113]), whereas for the commercial sample it is pure Cauchy along [110] and [113] but Voigtian along [012]. Thus the general formalism as outlined in previous sections holds.

4.2 Williamson–Hall plots

A simple qualitative information regarding the nature of the coherently diffracting domain (i.e. morphology, size–strain information) prior to any detailed analysis may be obtained on the basis of Williamson–Hall (WH) plot. Figure 2 shows the WH plot for the different samples. For both the as-prepared and annealed samples, b_F^* (in $\sin q$ scale) shows very small s dependence. A few scattered points in the high s region may be attributed to inaccuracy in pattern decomposition from overlapping reflections. It is further observed that the line connecting the two orders 012 and 024 have almost zero slope indicating negligible distortion along [012]. Small lattice distortions may be similarly predicted along [110] and [113]. This is also supported by the fact that for hhl type reflections b_F^* increases with the increase in l (e.g. 111

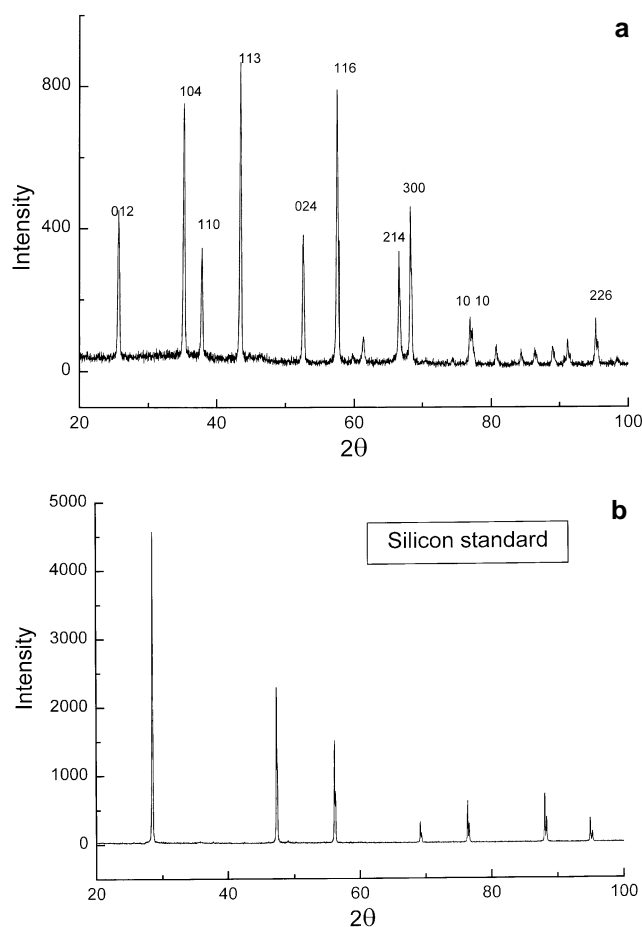


Figure 1. XRD patterns of **a.** α -Al₂O₃ (as-prepared) and **b.** standard Si sample.

and 22l reflections). It is further observed that $hk0$ type reflections yield a smaller intercept on the b -scale compared to the hkl type reflection implying anisotropic shape of the crystallites. The intercept of the WH plot gives the value of effective domain size. A lower intercept for annealed α -Al₂O₃ indicates an increase in the crystallite size, a further decrease in slope indicates release of strain.

Thus from the WH plots it can be inferred that both the as-prepared and annealed Al₂O₃ samples show shape anisotropy and in addition there is a small effect of lattice distortion. However, the lattice distortion decreases with annealing treatment. For the commercial Al₂O₃ sample a straight line could be drawn through all the points with negligible slope indicating that b_F^* is globally independent of s . Further, the points are scattered uniformly around the straight line indicating that line broadening is governed by small crystallite lacking significant shape anisotropy and with insignificant lattice distortion. It must be noted that WH plot is justified for only Cauchy type profiles. The present analysis of Al₂O₃ samples shows that the profiles are Voigtian on the contrary. However, WH plot is justified for purely qualitative purpose only.

4.3 Double-Voigt analysis for size and strain

The general conclusions obtained from the simple WH plot can be further substantiated by a detailed analysis.

Table 1. Values of Cauchy component (b_C) and Gaussian component (b_G) of integral breadth.

		b_C (deg.)	b_G (deg.)
Al ₂ O ₃	[012]	0.064	0.110
	[024]	0.081	0.120
Al ₂ O ₃ (800°C)	[012]	0.055	0.101
	[024]	0.058	0.115
Al ₂ O ₃ (C)	[012]	0.068	0.053
	[024]	0.077	0.151
Al ₂ O ₃	[110]	0.069	0.104
	[220]	0.156	0.378
Al ₂ O ₃ (800°C)	[110]	0.074	0.058
	[220]	0.221	0.122
Al ₂ O ₃ (C)	[110]	0.065	0.000
	[220]	0.117	0.000
Al ₂ O ₃	[113]	0.058	0.139
	[226]	0.244	0.246
Al ₂ O ₃ (800°C)	[113]	0.058	0.106
	[226]	0.212	0.201
Al ₂ O ₃ (C)	[113]	0.058	0.000
	[226]	0.135	0.000

Al₂O₃: α -Al₂O₃ as-prepared; Al₂O₃ (800°C): α -Al₂O₃ annealed at 800°C; Al₂O₃ (C): commercial α -Al₂O₃; b_C : Cauchy component of integral breadth; b_G : Gaussian component of integral breadth.

Assuming both the size and the strain broadened profiles are approximated by Voigt function, the Cauchy and the Gaussian components (b_{SC} , b_{SG} , b_{DC} , and b_{DG}) of the size (b_{SC} and b_{SG}) and strain (b_{DC} and b_{DG}) broadened profiles are separated as described in § 3.2. The results are given in table 2. It is observed from table 2 that in general both size and strain broadened profiles have Cauchy and Gaussian contributions. Whenever the true profiles were of Cauchy type the Gaussian components are set to be zero. For the commercial samples the size broadened profiles are generally Cauchy in nature indicating probably a broad size distribution. In case of as-prepared and annealed samples a significant Gaussian size contribution is noticed. This fact is not unnatural and has been predicted by several authors (e.g. Balzar and Ledbetter 1993).

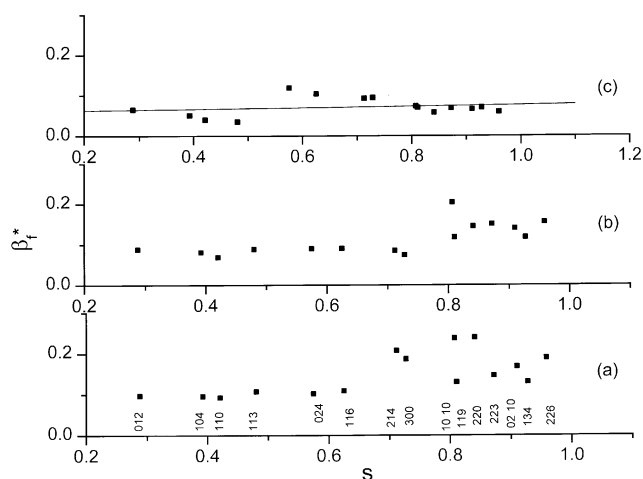


Figure 2. Variation of b_F^* vs s for (a) α -Al₂O₃ (as-prepared), (b) α -Al₂O₃ annealed (800°C) and (c) α -Al₂O₃ (commercial).

Table 2. Values of Cauchy and Gaussian components of size and strain.

	b_{dc} ($\times 10^4$)	b_{sc} ($\times 10^4$)	b_{sg} ($\times 10^4$)	b_{dg} ($\times 10^4$)
[012]				
Al ₂ O ₃	0.41	6.64	12.08	0.87
Al ₂ O ₃ (800°C)	0	6.23	10.96	2.04
Al ₂ O ₃ (C)	0.11	7.38	0	8.24
[110]				
Al ₂ O ₃	2.06	5.31	0	17.77
Al ₂ O ₃ (800°C)	3.74	4.17	3.73	4.97
Al ₂ O ₃ (C)	1.04	5.92	0	0
[113]				
Al ₂ O ₃	4.21	1.87	12.95	6.85
Al ₂ O ₃ (800°C)	3.37	2.74	9.46	6.07
Al ₂ O ₃ (C)	1.41	4.74	0	0

b_{dc} , b_{sc} : Cauchy components of strain and size of integral breadths, respectively, b_{dg} , b_{sg} : corresponding Gaussian components.

The size and strain Fourier coefficients according to the double-Voigt approach presented here is calculated according to (9). The microstructural parameters obtained from the Voigt generalization is listed in table 3. To compare the result and test the reliability of the method a direct Warren–Averbach/Stokes deconvolution method was applied to the Fourier coefficients as described by Enzo *et al* (1988) for several orders. The effective surface averaged domain size, D_s , calculated from the initial slope of the size Fourier coefficients and that obtained from the double-Voigt approach according to (10) and the rms microstrains (rmss) calculated at 100 Å are compared. Small ‘hook’ effect was observed in the size Fourier coefficients for the as-prepared and annealed samples. The ‘hook’ effect prevailed for both analytical double-Voigt and Warren–Averbach method indicating that the possible source is due to underestimation of the Cauchy component of the profiles. However, a non-existent hook effect in case of commercial samples measured and analysed in a similar way suggests that the significant Gaussian size contribution in the as-prepared samples could be related to sample processing history (viz. size distribution) and may have produced the observed ‘hook’ effect. The distribution functions calculated from the double-Voigt approach are compared for the different samples and the different crystallographic directions.

On comparing the results in table 3 a good agreement is observed between the domain sizes and microstrains calculated from WA and double-Voigt approach. Thus it may be inferred from the results that both the size and strain broadened profiles are Voigt in nature. This establishes the equivalence of WA and the proposed double-Voigt approaches in line-broadening studies. It is further

Table 3. Values of crystallite size and RMS strains from double-Voigt and Warren-Averbach analysis for α -Al₂O₃ powder.

	$D_{s(DV)}$ (Å)	$D_{s(WA)}$ (Å)	e_{dv} (10 ³)	e_{wa} (10 ³)
[012]				
Al ₂ O ₃	507	515	0.72	0.68
Al ₂ O ₃ (800°C)	880	704	0.28	0
Al ₂ O ₃ (C)	678	646	1.20	1.14
[110]				
Al ₂ O ₃	941	911	2.00	1.98
Al ₂ O ₃ (800°C)	1196	1067	1.54	1.50
Al ₂ O ₃ (C)	844	809	0.77	0.75
[113]				
Al ₂ O ₃	521	476	1.50	1.45
Al ₂ O ₃ (800°C)	680	617	1.32	1.30
Al ₂ O ₃ (C)	1055	1059	0.79	0.80

$D_{s(DV)}$, $D_{s(WA)}$: Crystallite size from double Voigt and Warren–Averbach analysis, respectively; e_{dv} , e_{wa} : corresponding RMS strains.

observed that even in cases where the true broadened profiles are Cauchy (e.g. commercial alumina samples), the correspondence is good and both size and strain broadened profiles are Cauchy in nature. The qualitative conclusions of WH analysis is also established. Along [012] negligible lattice distortions is confirmed from the actual measurements (rmss ~ 0.07% for as-prepared and ~ 0.03% for annealed sample), whereas the effect of lattice distortions along [110] and [113] is also clearly

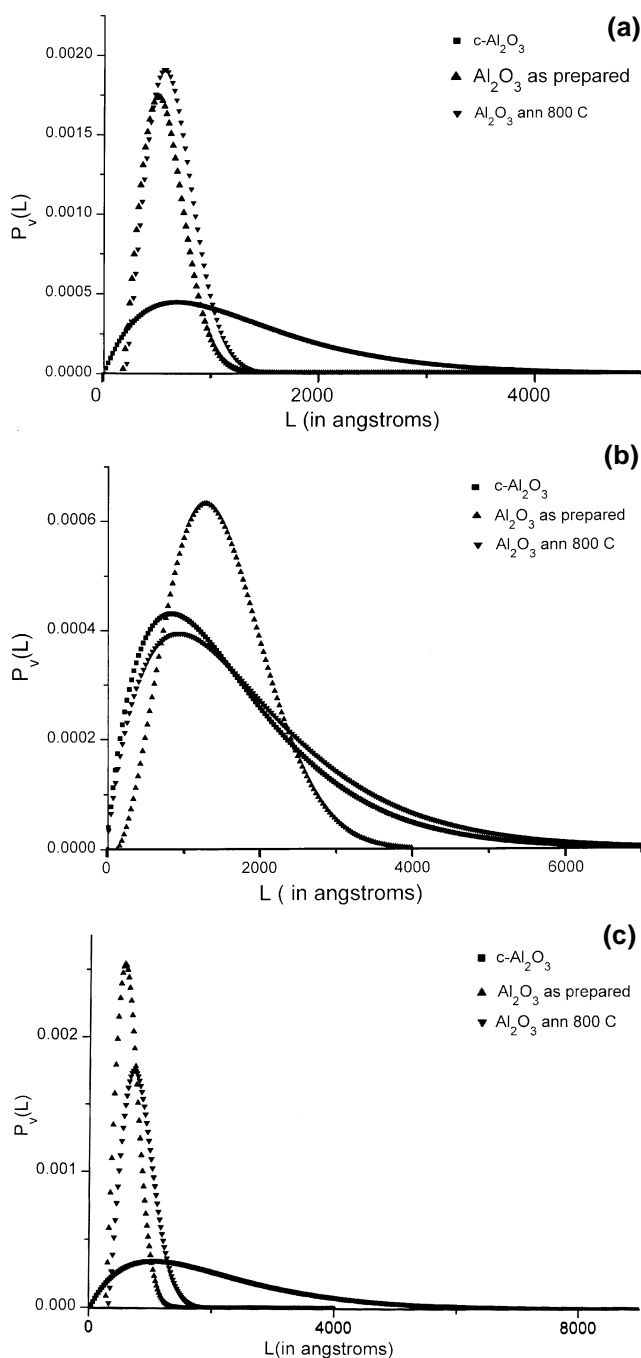


Figure 3. Variation of crystallite size distribution $P_v(L)$ with L : (a) [012], (b) [110] and (c) [113] directions.

Table 4. Values of crystallite size and RMS strain.

	D_v (Å)	D_{cc} (Å)	D_{cg} (Å)	D_{gg} (Å)	ϵ_{cc} ($\times 10^3$)	ϵ_{cg} ($\times 10^3$)	ϵ_{gg} ($\times 10^3$)
[012]							
Al ₂ O ₃	581	626	601	601	0.18	0.43	0.59
Al ₂ O ₃ (800°C)	635	665	655	655	0.06	0.23	0.33
Al ₂ O ₃ (C)	1355	4879	2783	1833	1.62	1.64	1.74
[110]							
Al ₂ O ₃	1068	+	+	+	3.03	3.20	2.60
Al ₂ O ₃ (800°C)	1482	+	+	+	1.58	1.58	1.53
Al ₂ O ₃ (C)	1687	+	+	+	0.37	0.42	0.50
[113]							
Al ₂ O ₃	631	1940	1184	912	1.41	1.44	1.59
Al ₂ O ₃ (800°C)	821	2727	1622	1186	1.23	1.25	1.35
Al ₂ O ₃ (C)	2101	5156	3240	2613	0.44	0.45	0.50

D_v : Crystallite size from volume distribution; D_{cc} , D_{cg} , D_{gg} : crystallite sizes from Cauchy–Cauchy, Cauchy–Gaussian, Gaussian–Gaussian components; ϵ_{cc} , ϵ_{cg} , ϵ_{gg} : corresponding RMS strains; +: Negative crystallite size.

established. The crystallite sizes along [012] and [113] do not differ much but along [110] the crystallite size is definitely larger and a significant lattice distortion (rms $\sim 0.2\%$) is noticed indicating both shape anisotropy and lattice distortion. The effect of lattice distortion is also negligible for the commercial alumina sample and varies between 0.07% to 0.1% for different directions.

The volume-weighted column-length distribution calculated from the size Fourier coefficients are shown in figure 3. The observed hook effect in the size Fourier coefficients leads to physically impossible negative value of distribution function for the small L values. The errors in the size Fourier coefficients for small L values may arise from the insufficiency in strain correction formula (12) and is mainly connected with high strain values and/or strain distribution departing from a Gaussian. In the present case small values of strains rule out such a possibility. The only remaining effect is the truncation effect which cuts off effectively the long tails of a Cauchy profile and may lead to hook effect. In our pattern decomposition scheme each profile is measured to sufficient extent and the truncation effect, if present is minimum. This establishes the fact that size broadened profile has significant Gaussian contribution. Thus within the experimental errors the distribution function may be assumed to be reliable. The distribution function $P_v(L)$ along both [012] and [113] is rather narrow for both as-prepared and annealed samples (figures 3a and c) and is almost identical, the only difference being that the maximum shifts to high L indicating an increase in the fraction of larger crystallites. This establishes that not only the effective domain size but also their distribution do not differ much. The commercial alumina sample shows a much wider distribution of column lengths in

both the directions and is clearly non-homogeneous in terms of domain sizes.

4.4 Comparison with integral breadth method

The volume weighted domain size obtained from the double-Voigt method was also compared with the multiple line integral breadth method (table 4). It is observed from table 4 that the values of the domain size is greatly overestimated when compared with the equivalent volume-weighted crystallite size calculated from the double-Voigt approach along [113] with moderate level of lattice distortion. Along [012] which shows least distortion effect the correspondence is better. In some cases negative or imaginary values of crystallite size was obtained (particularly along [110] for the as-prepared and annealed alumina samples) which is due to the fact that the ratio of integral breadths of the second and first order is greater than two. It is interesting to note that both WA/double Voigt analysis indicate significant amount of strain broadening along [110]. The above result clearly establishes the fact that neither of the multiple line integral breadth methods yields reliable results. The Cauchy–Cauchy assumption in particular produces maximum overestimation and the Gaussian–Gaussian assumption the least. Similar observation has been noted in previous studies (Balzar and Popovic 1996). The microstrains on the other hand do not show much scatter when compared with the rms microstrains (tables 3 and 4). This is probably due to the fact that lattice distortion is either small or absent altogether. Thus it can be concluded that when both size and strain broadened profiles are Voigtian which is generally the case in the present study,

neither simplified integral breadth methods yields reliable results.

5. Conclusions

(I) As-prepared α -Al₂O₃ shows in addition to size broadening a measurable amount of strain broadening. Annealing increases the crystallite size and decreases the strain. Commercial α -Al₂O₃ on the other hand shows prominent size broadening only.

(II) The assumption of Voigtian size and strain broadened profiles yields results comparable to Warren–Averbach method. Size broadened profiles contain significant Gaussian contribution for both as-prepared and annealed samples.

(III) The crystallite size distribution function shows that combustion technique is capable of yielding homogeneous and narrow particle size distribution and it is likely that a narrow size distribution is linked with a significantly Gaussian size broadened profile.

(IV) A final comparison with the integral breadth method yields a general conclusion that neither of the simplified methods yields reliable value of size and strain and the present double Voigt analysis may replace the earlier methods of analysis.

Acknowledgement

Two of the authors ((KS) and (PC)) acknowledge CSIR, New Delhi, for financial support.

References

- Balzar D and Ledbetter H 1993 *J. Appl. Cryst.* **26** 561
Balzar D and Popovic S 1996 *J. Appl. Cryst.* **29** 16
de Keijser Th H, Langford J I, Mittemeijer E J and Vogels A B P 1982 *J. Appl. Cryst.* **15** 308
Enzo S, Fagherazzi G, Benedetti A and Polizzi S 1988 *J. Appl. Cryst.* **21** 536
Langford J I 1980 *Accuracy in powder diffraction, NBS special publication, No. 567* (eds) S Block and C R Hubbard (Washington DC: National Bureau of Standards) p. 255
Langford J I 1992 *Accuracy in powder diffraction II, NIST special publication, No. 846* (eds) E Prince and J K Stalick (Washington DC: US Department of Commerce) p. 110
Luterotti L and Scardi P 1990 *J. Appl. Cryst.* **23** 246
Stokes A R 1948 *Proc. Phys. Soc. London* **61** 382
Warren B E and Averbach B L 1952 *J. Appl. Phys.* **23** 497
Warren B E 1969 *X-ray diffraction* (Reading, MA: Addison-Wesley)